# TWO-DIMENTIONAL DIFFUSION MODEL FOR DIFFUSE INK PAINTING

TOSIYASU L.KUNII
Faculty Computer&Information Sc.,
Hosei University,
Tokyo, 184-8584, Japan

GLEB V.NOSOVSKIJ
Faculty Mechanics&Mathematics,
Moscow State Univ.,
Moscow,119899, Russia

VLADIMIR L. VECHERININ
Faculty Mechanics&Mathematics,
Moscow State Univ.,
Moscow,119899, Russia

Recieved
Revised
Communicated by A.T.Fomenko

**Abstract**

In our previous work [1] the multidimensional diffusion model for computer animation of diffuse ink painting was suggested. In diffuse painting final image is a result of ink diffusion in absorbent paper. A straightforward diffusion model however is unable to provide very specific features of real diffuse painting. In particular, it can not explain the appearance of certain singularities in intensity of color in the image which are very important features of diffuse ink painting. A multidimensional diffusion model which we propose proves to provide the intensity distributions very similar to those in real images.

In [1] only few calculations in the case of a circle as an initial zone were presented. Now we modify the model and present the results of more accurate calculations for an initial zone of arbitrary shape.

*Keywords* : Multidimensional diffusion processes, Nijimi, Colloidal liquid, Computer animation.

## 1 Introduction

Diffuse ink painting (in Japanese - 'Sumie') is a kind of ink painting on a special paper with high absorbency. The ink used in 'Sumie' is a colloidal liquid which consists from water and solid particles of carbon distributed in it. Glue is also added. Diffuse ink painting phenomenon is a new topic in

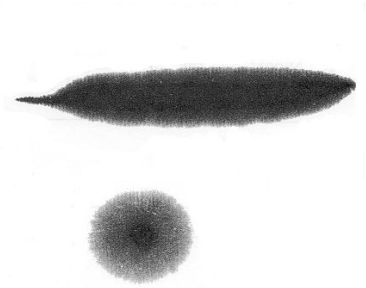

Figure 1: Examples of diffuse ink painting

computer graphics. Although some previous papers discussed the modeling of painting strokes ([5, 4, 7]) and liquid flow ([3, 6]), the diffuse ink effect was not analyzed.

When a drop of diffuse ink falls on the surface of highly absorbent paper, it begins to spread throughout the paper. As a result of this process, the final image appears to be sufficiently bigger then the initial zone to which the ink was directly applied. See Fig. 1.

The remarkable feature of diffuse ink image is a kind of black border which appears along the edge of the *initial zone* (i.e. zone where ink was directly applied to paper). One can see that the intensity of color along the border of the initial zone is higher then inside the zone.

Outside the initial zone there finally appears a sufficiently large *gray zone* with not very high, but more or less homogeneous intensity of color. The border of this zone appears to be rather irregular, 'feathery'. This gray zone is one where ink is not directly applied to paper. Carbon particles collect there as a result of diffusion.

We will call such distribution of color intensity in the image as *initial zone - black border - gray zone distribution.*

The typical intensity diagram of diffuse ink image (i.e. the diagram of surface density of carbon particles within a certain point of the image) is shown in Fig. 3. This figure correspond to the case when ink was initially applied in a central symmetrical area on the paper (i.e initial zone is a disk). Note, that in this case, there appears a peak in intensity, right in the center.

This article is concerned with a problem of numerical simulation and computer animation of the phenomena of diffuse ink painting. In order to solve this problem authors suggested in [1] a mathematical model of a 2-dimensional diffusion process with the above mentioned initial zone - black border - gray zone intensity distribution in the image area (see Fig. 3).

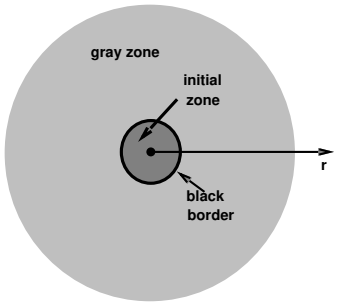


Figure 2: Distribution of color intensity in a stain which was made on the paper by diffuse ink. Three zones of different intensity appear in the image: 1. initial zone where ink was directly applied to paper; 2. black border - a dark line along the border of the initial zone; 3. gray zone - the area where solid particles of the ink collect as a result of diffusion.

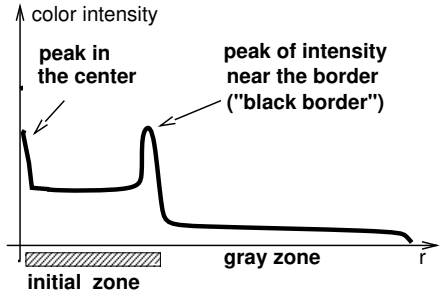


Figure 3: Typical diagram of surface density of carbon particles within a certain point of the image for real 'Sumie' painting. The horizontal axis corresponds to the distance $r$ of a certain point from the center of the image, and vertical axis represents the value of gray color intensity within that point.

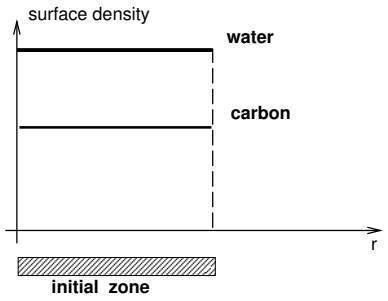


Figure 4: Initial distribution of water and carbon in a round stain made by a drop of diffuse ink on the surface of the paper.

## 2 A phenomenological model for initial zone - black border - gray zone distribution of intensity in diffuse ink painting image

In this section will briefly remember the phenomenological model for diffuse ink painting from [1].

Let us assume that the temperature is constant. Then the diffusion coefficient for carbon particles depends only on a concentration of carbon particles in water. The higher this concentration is - the slower diffusion might be. But the concentration of carbon in water changes with time in each point of the image. Thus, the diffusion coefficient for the motion of carbon particles can strongly depend on time and on the point of the image.

Consider an initial distribution of water and carbon particles density as shown in Fig. 4.

Due to spread of water outside of initial zone, the density of carbon in water will decrease inside this zone. The sharpest decrease of this density will occur near the bor der of initial zone because gradient of density function is maximal there. Consequently, it seems that distribution of water density would soon become like the distribution shown in Fig. 5.

As to carbon particles, they can diffuse only in water (not in the paper itself). As mentioned above, the diffusion coefficient for the motion of carbon particles can depend on a concentration of these particles in water. Diffusion slows down when concentration is too high.

After diffusion starts, the density of water along the border of initial zone begins to fall very rapidly with time. Consequently, the concentration of carbon particles in water (i.e. ratio carbon to water) rises sharply along

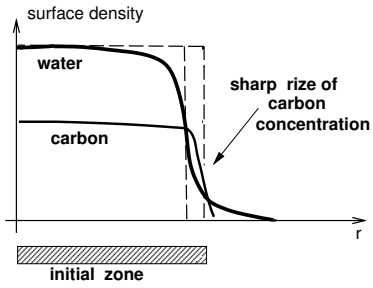


Figure 5: Distribution of water and carbon in the stain made by diffuse ink on the surface of the paper after the diffusion process starts.

the boundary of initial zone. Thus, along this boundary diffusion of carbon particles can sharply slow down because of high local concentration of carbon particles with respect to the local concentration of water. It can result in the appearance of a *barrier* for carbon particles near the border of initial zone. Many carbon particles which diffuse to the boundary of initial zone from inner parts of this zone, begin to slow down there and can not leave the vicinity of the border. After water dries up they remain near the boundary. That is how *black boundary* effect may occur.

Some carbon particles which are able to overcome this barrier, appear outside the initial zone. Those particles immediately fall into a zone where there is much more water than carbon. Although there might be little water outside the initial zone, the decrease in the number of carbon particles can be even greater than decrease of water density. In this case, concentration of carbon particles in water appears to be sufficiently low outside of initial zone which results in a diffusion with maximal rate for carbon outside the initial zone. Carbon particles there diffuse freely in water and draw a *gray zone* around initial zone. In this gray zone, intensity of gray color will be approximately constant. Due to the effects described above, the gray zone will be separated from initial zone by a dark line - *black boundary*. Therefore the density distribution function will look as shown on Fig. 3.

# 3 Continuous mathematical model and it's discrete approximation

Let us choose some Cartesian coordinate system $(x, y)$ on the surface of the paper. Time variable will be denoted by $t$. Consider a touch of brush with

diffuse ink to the surface of the paper at the moment $t = 0$. Assume that at the first moment $t = 0$, densities of water and carbon particles are constants $C_1$ and $C_2$ respectively, in the initial zone $D_0$ (i.e. in the area where brush touched the paper).

Let $g(x, y, t)$ denote the surface density of water in the point $(x, y)$ on the paper at the moment $t$, $(t >= 0)$. Similarly, let us denote by $f(x, y, t)$ the surface density of carbon particles on the paper.

At the beginning, the distributions of water and carbon in the paper are as follows

$$g(x, y, 0) = C_1, \quad f(x, y, 0) = C_2 \qquad (x, y) \in D_0;$$

$$f(x, y, 0) = 0, \quad f(x, y, 0) = 0 \qquad (x, y) \notin D_0.$$

In [1] we suggested the model in which the densities of water and carbon particles on the paper surface change with time according to the following system of differential equations:

$$\begin{aligned} \frac{\partial g}{\partial t} &= \nabla(a^2 \nabla g) - \frac{1}{\tau} g + p\frac{\partial g}{\partial x} + q\frac{\partial g}{\partial y}, \\ \frac{\partial f}{\partial t} &= \nabla\left(Z\left(\frac{g}{f}\right)\nabla f\right). \end{aligned} \tag{1}$$

Boundary conditions are zero as point $(x, y)$ tends to infinity. Practically we assume that a sheet of paper is large enough so that water will dry up before reaching the edge of the paper.

In above equations the coefficient $\frac{1}{\tau}$ characterizes the speed of drying process of the water. Coefficients $p$ and $q$ determine a flow of water on the surface of paper. Such flow may be present due to special structure of the paper or due to gravitational effects in the case when the sheet of paper is fixed not horizontally. Parameter $a$ determines the diffusion of water on the surface of the paper. If the paper structure is not homogeneous then $a$ will be not constant. It can depend on coordinates $(x, y)$ in the case, for example, when the paper was manufactured in such a way that there exist some typical directions of paper fibers, which are different in different parts of the paper sheet.

The choice of function $Z(\frac{g}{f})$ is important. This function determines how the diffusion rate of carbon particles depends on the concentration of carbon in the water. Our calculations show that properties of intensity distribution in the final image can strongly depend on the shape of the curve $y = Z(x)$.

We performed a number of numerical experiments in order to determine the appropriate shape of function $Z$. It turns out that the initial zone -

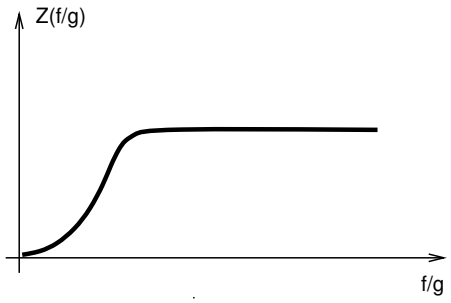


Figure 6: Behavior of a function $Z(\frac{g}{f})$ which results in appearance of initial zone - black boundary - gray zone distribution phenomenon in diffuse ink painting simulation.

black boundary - gray zone distribution phenomenon occurs in the case when function $Z$ is concave in the interval of it's rise (i.e. in the vicinity of zero, because for sufficiently large values of argument, function $Z$ should be constant: rate of diffusion for the motion of carbon particles will not change when water is added provided that there was already enough water).

In order to obtain computer animation of evolution of diffuse ink image on the paper, we solve the system of partial differential equations (1) numerically on a grid.

Assume that a sheet of paper is placed horizontally and that the paper is homogeneous: $p, q = 0$ and $a = const$. In this case the system (1) could be written in a follows way

$$\begin{aligned} \frac{\partial g}{\partial t} &= a^2 \triangle g - \lambda g, \\ \frac{\partial f}{\partial t} &= \nabla \left( Z\left(\frac{g}{f}\right) \nabla f \right). \end{aligned} \tag{2}$$

Here we use the following notations:
$g = g(x, y, t)$ - the surface density of water,
$f = f(x, y, t)$ - the surface density of carbon,
$\lambda$ - rate of water drying,
$a$ - rate of water diffusion,
$Z = Z(g/f)$ - a given function, which determines the dependence of carbon diffusion rate on the local concentration of the carbon in water in a certain point on the paper. In our calculations we choose function $Z$ as follows:

$$Z(g/f) = \begin{cases} \frac{Z_0\left(1-\cos(\frac{\pi}{Z_1}\frac{g}{f})\right)}{2}, & \text{when } \frac{g}{f} \le Z_1 \\ Z_0, & \text{when } \frac{g}{f} > Z_1 \end{cases}$$

where $Z_0, Z_1$ are some constants.

We will approximate the quasi-linear system (2) on a discrete grid of the size $N \times N$, presenting the square area on the paper. The space step of the grid is denoted by $h$, the time step is denoted by $\tau$. We use the implicit method of discretization with alternating direction [8]. Finally, we obtain the following system of linear equations on the grid. Here $0 \le i, j \le N$.

$$\begin{aligned} \frac{g_{ij}^{n+\frac{1}{2}} - g_{ij}^{n}}{\tau/2} &= \frac{g_{i-1,j}^{n+\frac{1}{2}} - 2g_{ij}^{n+\frac{1}{2}} + g_{i+1,j}^{n+\frac{1}{2}} + g_{i,j-1}^{n} - 2g_{i,j}^{n} + g_{i,j+1}^{n}}{h^2}a^2 - \lambda g_{ij}^{n+\frac{1}{2}}, \\ \frac{g_{ij}^{n+1} - g_{ij}^{n+\frac{1}{2}}}{\tau/2} &= \frac{g_{i-1,j}^{n+\frac{1}{2}} - 2g_{ij}^{n+\frac{1}{2}} + g_{i+1,j}^{n+\frac{1}{2}} + g_{i,j-1}^{n+1} - 2g_{i,j}^{n+1} + g_{i,j+1}^{n+1}}{h^2}a^2 - \lambda g_{ij}^{n+1}, \end{aligned} \tag{3}$$

$$\begin{aligned} \frac{f_{ij}^{n+\frac{1}{2}} - f_{ij}^{n}}{\tau/2} &= \frac{Z_{1;ij}^{n+\frac{1}{2}} f_{i-1,j}^{n+\frac{1}{2}} - (Z_{1;ij}^{n+\frac{1}{2}} + Z_{1;i+1,j}^{n+\frac{1}{2}}) f_{ij}^{n+\frac{1}{2}} + Z_{1;i+1,j}^{n+\frac{1}{2}} f_{i+1,j}^{n+\frac{1}{2}}}{h^2} \\ &+ \frac{Z_{2;ij}^{n} f_{i,j-1}^{n} - (Z_{2;ij}^{n} + Z_{2;i,j+1}^{n}) f_{i,j}^{n} + Z_{2;i,j+1}^{n} f_{i,j+1}^{n}}{h^2}, \\ \frac{f_{ij}^{n+1} - f_{ij}^{n+\frac{1}{2}}}{\tau/2} &= \frac{Z_{1;ij}^{n+\frac{1}{2}} f_{i-1,j}^{n+\frac{1}{2}} - (Z_{1;ij}^{n+\frac{1}{2}} + Z_{1;i+1,j}^{n+\frac{1}{2}}) f_{ij}^{n+\frac{1}{2}} + Z_{1;i+1,j}^{n+\frac{1}{2}} f_{i+1,j}^{n+\frac{1}{2}}}{h^2} \\ &+ \frac{Z_{2;ij}^{n+1} f_{i,j-1}^{n+1} - (Z_{2;ij}^{n+1} + Z_{2;i,j+1}^{n+1}) f_{i,j}^{n+1} + Z_{2;i,j+1}^{n+1} f_{i,j+1}^{n+1}}{h^2}. \end{aligned} \tag{4}$$

In the above equations we use the following notations:

$f_{i,j}^{n}$ and $g_{i,j}^{n}$ denote the approximations for the functions $f$ and $g$ respectively in the node $(i,j)$ of the grid at the time layer $n$;

$f_{i,j}^{n+\frac{1}{2}}$ and $g_{i,j}^{n+\frac{1}{2}}$ denote the approximations for the functions $f$ and $g$ respectively in the node $(i,j)$ at the intermediate time layer $n+\frac{1}{2}$;

$Z_{1;ij}^{k}, Z_{2;ij}^{k}$ denote the values:

$$\begin{aligned} Z_{1;ij}^{k} &= \frac{1}{2}\left(Z\left(\frac{g_{i-1,j}^{k}}{f_{i-1,j}^{k}}\right) + Z\left(\frac{g_{i,j}^{k}}{f_{i,j}^{k}}\right)\right), \\ Z_{2;ij}^{k} &= \frac{1}{2}\left(Z\left(\frac{g_{i,j-1}^{k}}{f_{i,j-1}^{k}}\right) + Z\left(\frac{g_{i,j}^{k}}{f_{i,j}^{k}}\right)\right). \end{aligned} \tag{5}$$

To solve the system (4) it is necessary to know the values $Z_{ij}$ on the future level $n+\frac{1}{2}$. These values were determined approximately in the calculation process by the following recursive method.

1) At first step we calculate $f_{i,j}^{n+\frac{1}{2}}$ from (4) using $Z_{ij}^{n}$ instead of $Z_{ij}^{n+\frac{1}{2}}$ and $g_{i,j}^{n+\frac{1}{2}}$ from (3). Using these values we calculate $Z_{i,j}^{n+\frac{1}{2}}$ from (5).

2) Then using obtained values of $Z_{i,j}^{n+\frac{1}{2}}$ we find $f_{i,j}^{n+\frac{1}{2}}$ from (4) once more.

3) Using new values of $f_{i,j}^{n+\frac{1}{2}}$ we find again the values of $Z_{i,j}^{n+\frac{1}{2}}$ from (5).

4) With new values of $Z_{i,j}^{n+\frac{1}{2}}$ we go to step 2). This cycle was repeated 2-3 times until the values of $f_{i,j}^{n+\frac{1}{2}}$ become stable.

In order to solve the system of equations (3)(4)) we will rewrite it in the follows form:

$$\begin{aligned}
\frac{a^2}{h^2}g_{i-1,j}^{n+\frac{1}{2}} &- \left(\frac{2a^2}{h^2}+\lambda+\frac{2}{\tau}\right)g_{ij}^{n+\frac{1}{2}}+\frac{a^2}{h^2}g_{i+1,j}^{n+\frac{1}{2}}= \\
&= -\left(\frac{2g_{ij}^{n}}{\tau}+\frac{a^2}{h^2}(g_{i,j-1}^{n}-2g_{i,j}^{n}+g_{i,j+1}^{n})\right), \\
\frac{a^2}{h^2}g_{i,j-1}^{n+1} &- \left(\frac{2a^2}{h^2}+\lambda+\frac{2}{\tau}\right)g_{ij}^{n+1}+\frac{a^2}{h^2}g_{i,j+1}^{n+1}= \\
&= -\left(\frac{2g_{ij}^{n+\frac{1}{2}}}{\tau}+\frac{a^2}{h^2}(g_{i-1,j}^{n+\frac{1}{2}}-2g_{i,j}^{n+\frac{1}{2}}+g_{i+1,j}^{n+\frac{1}{2}})\right). \qquad (6)
\end{aligned}$$

$$\begin{aligned}
\frac{Z_{1;ij}^{n+\frac{1}{2}}}{h^2}f_{i-1,j}^{n+\frac{1}{2}} &- \left(\frac{2}{\tau}+\frac{Z_{1;ij}^{n+\frac{1}{2}}+Z_{1;i+1,j}^{n+\frac{1}{2}}}{h^2}\right)f_{ij}^{n+\frac{1}{2}}+\frac{Z_{1;i+1,j}^{n+\frac{1}{2}}}{h^2}f_{i+1,j}^{n+\frac{1}{2}}= \\
&= -\left(\frac{2f_{ij}^{n}}{\tau}+\frac{Z_{2;ij}^{n}f_{i,j-1}^{n}-(Z_{2;ij}^{n}+Z_{2;i,j+1}^{n})f_{ij}^{n}+Z_{2;i,j+1}^{n}f_{i,j+1}^{n}}{h^2}\right) \\
\frac{Z_{2;ij}^{n+1}}{h^2}f_{i,j-1}^{n+1} &- \left(\frac{2}{\tau}+\frac{Z_{2;ij}^{n+1}+Z_{2;i,j+1}^{n+1}}{h^2}\right)f_{ij}^{n+1}+\frac{Z_{2;i,j+1}^{n+1}}{h^2}f_{i,j+1}^{n+1}= \\
&= -\left(\frac{2f_{ij}^{n+\frac{1}{2}}}{\tau}+\frac{Z_{1;ij}^{n+\frac{1}{2}}f_{i-1,j}^{n+\frac{1}{2}}-(Z_{1;ij}^{n+\frac{1}{2}}+Z_{1;i+1,j}^{n+\frac{1}{2}})f_{ij}^{n+\frac{1}{2}}+Z_{2;i+1,j}^{n+\frac{1}{2}}f_{i+1,j}^{n+\frac{1}{2}}}{h^2}\right)
\end{aligned} \qquad (7)$$

To simplify the formulas we will use the following notations:

$$
\begin{aligned}
A &= B = \frac{a^2}{h^2}, \qquad C = \frac{2a^2}{h^2} + \lambda + \frac{2}{\tau},\\
G^n_{1;ij} &= \frac{2g^n_{ij}}{\tau} + \frac{a^2}{h^2}(g^n_{i,j-1} - 2g^n_{i,j} + g^n_{i,j+1}),\\
G^{n+\frac{1}{2}}_{2;ij} &= \frac{2g^{n+\frac{1}{2}}_{ij}}{\tau} + \frac{a^2}{h^2}(g^{n+\frac{1}{2}}_{i-1,j} - 2g^{n+\frac{1}{2}}_{i,j} + g^{n+\frac{1}{2}}_{i+1,j}),\\
A^{n+\frac{1}{2}}_{1;ij} &= \frac{Z^{n+\frac{1}{2}}_{1;ij}}{h^2}, \qquad B^{n+\frac{1}{2}}_{1;ij} = \frac{Z^{n+\frac{1}{2}}_{1;i+1,j}}{h^2}, \qquad (8)\\
C^{n+\frac{1}{2}}_{1;ij} &= \frac{2}{\tau} + \frac{Z^{n+\frac{1}{2}}_{1;ij} + Z^{n+\frac{1}{2}}_{1;i+1,j}}{h^2}, \qquad (9)\\
F^{n+\frac{1}{2}}_{1;ij} &= \frac{2f^n_{ij}}{\tau} + \frac{Z^n_{2;ij}f^n_{i,j-1} - (Z^n_{2;ij} + Z^n_{2;i,j+1})f^n_{ij} + Z^n_{2;i,j+1}f^n_{i,j+1}}{h^2},\\
A^{n+1}_{2;ij} &= \frac{Z^{n+1}_{2;ij}}{h^2}, \qquad B^{n+1}_{2;ij} = \frac{Z^{n+1}_{2;i,j+1}}{h^2}, \qquad (10)\\
C^{n+1}_{2;ij} &= \frac{2}{\tau} + \frac{Z^{n+1}_{2;ij} + Z^{n+1}_{2;i,j+1}}{h^2}, \qquad (11)\\
F^{n+1}_{2;ij} &= \frac{2f^{n+\frac{1}{2}}_{ij}}{\tau} + \frac{Z^{n+\frac{1}{2}}_{1;ij}f^{n+\frac{1}{2}}_{i-1,j} - (Z^{n+\frac{1}{2}}_{1;ij} + Z^{n+\frac{1}{2}}_{1;i+1,j})f^{n+\frac{1}{2}}_{ij} + Z^{n+\frac{1}{2}}_{2;i+1,j}f^{n+\frac{1}{2}}_{i+1,j}}{h^2}.
\end{aligned}
$$

With these notations the system (6)(7) obtains the form:

$$
\begin{aligned}
Ag^{n+\frac{1}{2}}_{i-1,j} - Cg^{n+\frac{1}{2}}_{ij} + Bg^{n+\frac{1}{2}}_{i+1,j} &= -G^n_{1;ij},\\
Ag^{n+1}_{i,j-1} - Cg^{n+1}_{ij} + Bg^{n+1}_{i,j+1} &= -G^{n+\frac{1}{2}}_{2;ij} \qquad (12)\\
A^{n+\frac{1}{2}}_{1;ij}f^{n+\frac{1}{2}}_{i-1,j} - C^{n+\frac{1}{2}}_{1;ij}f^{n+\frac{1}{2}}_{ij} + B^{n+\frac{1}{2}}_{1;ij}f^{n+\frac{1}{2}}_{i+1,j} &= -F^n_{1;ij},\\
A^{n+1}_{2;ij}f^{n+1}_{i,j-1} - C^{n+1}_{2;ij}f^{n+1}_{ij} + B^{n+1}_{2;ij}f^{n+1}_{i,j+1} &= -F^{n+\frac{1}{2}}_{2;ij} \qquad (13)
\end{aligned}
$$

The initial conditions for the system (12)(13) are defined by the form of the initial stain $D_{initial}$, the density of ink in $D_{initial}$, and the assumption that the sheet of paper is large enough and therefore the stain will not diffuse to the edge of paper.

$$
\begin{aligned}
g^n_{ij} &= 0, \quad f^n_{ij} = 0, \qquad \forall n, \quad i = 0, i = N, j = 0, j = N;\\
g^0_{ij} &= w, \quad f^0_{ij} = c, \qquad i, j \in D_{initial};\\
g^0_{ij} &= 0, \quad f^0_{ij} = 0, \qquad i, j \notin D_{initial};
\end{aligned}
$$

Here $w$ denotes the initial quantity of water and $c$ denotes the initial quantity of carbon in a pixel of the grid in the initial stain area $D_{initial}$.

The solution of the system (12) for water density for the time layer $(n+1)$ is obtained by the follows numerical procedure (see [8]).

At first step, using already calculated values of $g_{ij}^{n}$ on the time layer $n$, for each fixed $1 \leq j \leq N-1$ we obtain all values $\{g_{ij}^{n+\frac{1}{2}}, i = N-1, \ldots, 1\}$ on the intermediate time layer $n+\frac{1}{2}$ :

$$\begin{aligned} g_{Nj}^{n+\frac{1}{2}} &= 0; \\ g_{ij}^{n+\frac{1}{2}} &= \alpha_{i+1}^{1} g_{i+1,j}^{n+\frac{1}{2}} + \beta_{i+1}^{1}, \quad i = N-1, N-2, \ldots 1, \end{aligned}$$

where

$$\begin{aligned} \alpha_1^1 &= 0; \qquad \alpha_{i+1}^1 = \frac{B}{(C - \alpha_i^1 A)}; \qquad i = 1, \ldots, N-1; \\ \beta_1^1 &= 0; \qquad \beta_{i+1}^1 = \frac{A\beta_i^1 + G_{1;ij}^n}{C - \alpha_i^1 A} \qquad i = 1, \ldots, N-1; \end{aligned}$$

Then for each fixed $1 \leq i \leq N-1$ we obtain all values $\{g_{ij}^{n+1}, j = N-1, \ldots, 1\}$ on the time layer $n+1$ :

$$\begin{aligned} g_{iN}^{n+1} &= 0; \\ g_{ij}^{n+1} &= \alpha_{j+1}^{2} g_{i,j+1}^{n+1} + \beta_{j+1}^{2}, \quad j = N-1, N-2, \ldots 1. \end{aligned}$$

where

$$\begin{aligned} \alpha_1^2 &= 0; \qquad \alpha_{j+1}^2 = \frac{B}{(C - \alpha_j^2 A)}; \qquad j = 1, \ldots, N-1; \\ \beta_1^2 &= 0; \qquad \beta_{j+1}^2 = \frac{A\beta_j^2 + G_{2;ij}^{n+\frac{1}{2}}}{C - \alpha_j^2 A} \qquad j = 1, \ldots, N-1; \end{aligned}$$

After the determination of water density on time layer $n+1$, the density of carbon on the same layer is obtained from the system (13). The numerical procedure for carbon is given by similar formulas. But now we need to use the additional recursive procedure which was mentioned above. Of course it is possible to change the system (13) to a more simple standard form, so that it's solution could be obtained without recursion. But the approach

which we use improves the accuracy of the result in the case when function $Z$ is nonlinear ([8]).

At the beginning, for each fixed $1 \le j \le N-1$ we calculate first-step approximations for the values $\{f_{ij}^{n+\frac{1}{2}}, i = N-1, \dots, 1\}$ on the intermediate time layer $n+\frac{1}{2}$ by the formulas:

$$\begin{aligned} f_{Nj}^{n+\frac{1}{2}} &= 0; \\ f_{ij}^{n+\frac{1}{2}} &= \alpha_{i+1}^1 f_{i+1,j}^{n+\frac{1}{2}} + \beta_{i+1}^1, \quad i = N-1, N-2, \dots 1, \end{aligned}$$

where

$$\begin{aligned} \alpha_1^1 &= 0; \qquad \alpha_{i+1}^1 = \frac{B_{1;i,j}^{n+\frac{1}{2}}}{(C_{1;i,j}^{n+\frac{1}{2}} - \alpha_i^1 A_{1;i,j}^{n+\frac{1}{2}})}; \qquad i = 1, \dots, N-1; \\ \beta_1^1 &= 0; \qquad \beta_{i+1}^1 = \frac{A_{1;i,j}^{n+\frac{1}{2}} \beta_i^1 + F_{1;ij}^n}{C_{1;i,j}^{n+\frac{1}{2}} - \alpha_i^1 A_{1;i,j}^{n+\frac{1}{2}}} \qquad i = 1, \dots, N-1; \end{aligned} \tag{14}$$

At the first step the coefficients $\alpha_{i+1}^1, \beta_{i+1}^1$ are calculated not on the time layer $n+\frac{1}{2}$, as it is required by the system (13), but on the time layer $n$. It means that $A_{1;i,j}^n, B_{1;i,j}^n, C_{1;i,j}^n$ in (14) are initially determined by formulas (8)(9) with $Z_{\cdot}^{n+\frac{1}{2}}$ replaced by $Z_{\cdot}^n$. As a result we obtain first-step approximations for $f_{ij}^{n+\frac{1}{2}}$. Then we use them to calculate more accurate values of $Z_{\cdot}^{n+\frac{1}{2}}$. Next, we repeat the same calculations of $f_{ij}^{n+\frac{1}{2}}$ using new values of $Z_{\cdot}^{n+\frac{1}{2}}$. This cycle is repeated several (usually 2-3) times.

After this, using the same recursive procedure, for each fixed $1 \le i \le N-1$ we obtain all values $\{f_{ij}^{n+1}, j = N-1, \dots, 1\}$ on the time layer $n+1$ :

$$\begin{aligned} f_{iN}^{n+1} &= 0; \\ f_{ij}^{n+1} &= \alpha_{j+1}^2 g_{i,j+1}^{n+1} + \beta_{j+1}^2, \quad j = N-1, N-2, \dots 1. \end{aligned}$$

where

$$\begin{aligned} \alpha_1^2 &= 0; \qquad \alpha_{j+1}^2 = \frac{B_{2;i,j}^{n+\frac{1}{2}}}{(C_{2;i,j}^{n+\frac{1}{2}} - \alpha_j^2 A_{2;i,j}^{n+\frac{1}{2}})}; \qquad j = 1, \dots, N-1; \\ \beta_1^2 &= 0; \qquad \beta_{j+1}^2 = \frac{A_{2;i,j}^{n+\frac{1}{2}} \beta_j^2 + F_{2;ij}^{n+\frac{1}{2}}}{C_{2;i,j}^{n+\frac{1}{2}} - \alpha_j^2 A_{2;i,j}^{n+\frac{1}{2}}} \qquad j = 1, \dots, N-1. \end{aligned}$$

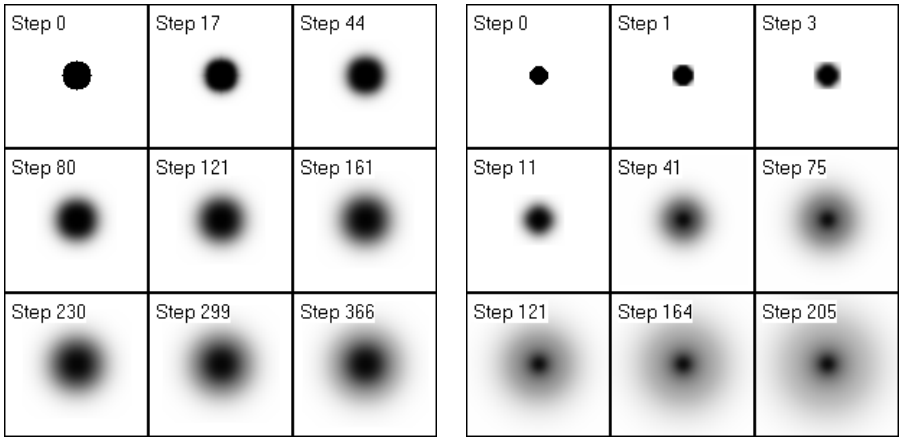


Figure 7: Two time-sequences of images of a round black stain, produced on the paper by a drop of diffuse ink. On the left: $a^2 = 1; \lambda = 0.05; Z_0 = Z_1 = 0.5$; initial quantity of water $w = 3$; quantity of carbon $c = 0.5$. On the right: $a^2 = 0.02; \lambda = 0.1; Z_0 = Z_1 = 2.5; w = 3; c = 0.5$. Computer animation.

All calculations are then repeated on the next time layer.

## 4 Results of computer simulation

Fig. 7 shows two results of calculations in the case of round stain which was made on the paper by a drop of diffuse ink. Model parameters for these two images have different values which results in their different appearance. Water and carbon were initially distributed uniformly in the stain. Calculations were made on the $300 \times 300$ pixels grids, initial diameter of the stain was 20-30 pixels. A initial zone - black boundary - gray zone distribution of color intensity could be observed on this picture.

Fig. 8 and Fig. 9 show the results of calculations for several initial zones of different shape. Values of parameters of the model were chosen here as follows: $a^2 = 0.02; \lambda = 0.1; Z_0 = Z_1 = 2.5$; initial quantity of water in the stain $w = 3$; quantity of carbon in the stain $c = 2$. Water and carbon in the stain are initially distributed uniformly. Calculations were made on the $450 \times 450$ pixels grids.

Next figures present several examples of calculations which show how the variation of model parameters changes the resulting image.

Fig. 10 and Fig. 11 consist from several pictures. Each picture shows the sequence of images produced by the computer simulation. From picture

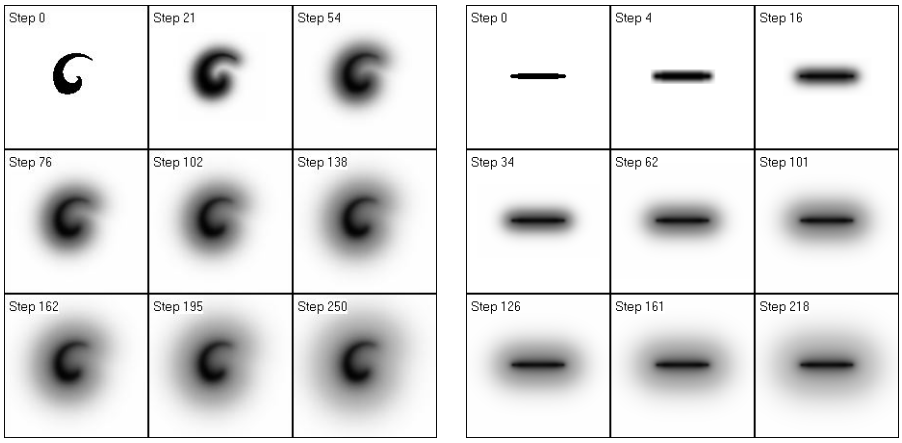


Figure 8: Time-sequences of images of initial stains of different shapes.I. Computer simulation.

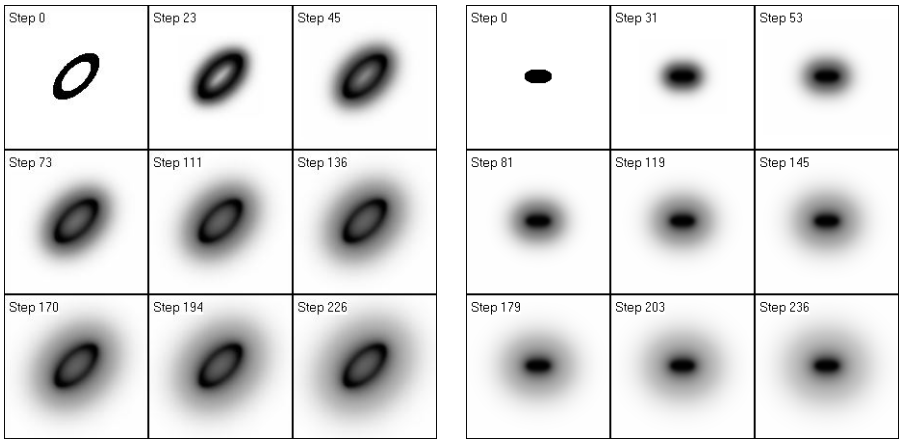


Figure 9: Time-sequences of images of initial stains of different shapes.II. Computer simulation.

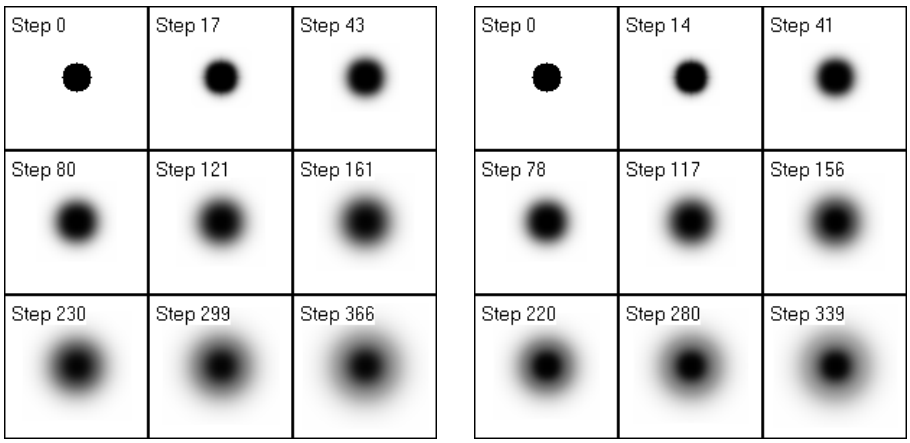


Figure 10: Changing of the resulting image when the water diffusion rate parameter $a^2$ decreases. Left picture: $a^2 = 0.5$. Right picture: $a^2 = 0.1$ Computer simulation.

to picture the water diffusion rate parameter $a^2$ decreases from the value $a^2 = 0.5$ to the value $a^2 = 0.005$. All other parameters keep constant values: $\lambda = 0.1$; $Z_0 = Z_1 = 0.5$; initial quantity of water in the stain $w = 3$; quantity of carbon in the stain $c = 0.5$. Water and carbon are initially distributed uniformly. Calculations were made on the $300 \times 300$ pixels grids.

Fig. 12 and Fig. 13 show several pictures produced by computer simulation with increasing rate of water drying $\lambda$. The value of $\lambda$ changes from $\lambda = 0.05$ to $\lambda = 0.4$. All other parameters keep constant values: $a^2 = 0.02$; $Z_0 = Z_1 = 2.5$; initial quantity of water $w = 3$; quantity of carbon $c = 1$. Water and carbon are initially distributed uniformly. Calculations were made on the $450 \times 450$ pixels grids.

Fig. 14 and Fig. 15 show a number of pictures produced by computer simulation with increasing quantity of carbon in the ink. The value of carbon quantity parameter $c$ changes here from $c = 0.5$ to $c = 5$. All other parameters keep constant values: $a^2 = 0.03$; $\lambda = 0.1$, $Z_0 = Z_1 = 2.5$; $w = 3$. Water and carbon are initially distributed uniformly. Calculations were made on the $450 \times 450$ pixels grids.

Finally, on Fig. 16 we present a number of pictures produced by computer simulation with increasing parameters $Z_0, Z_1$. All other parameters keep constant values: $a^2 = 1$; $\lambda = 0.05, w = 3, c = 0.5$. Water and carbon are initially distributed uniformly. Calculations were made on the $300 \times 300$ pixels grids.

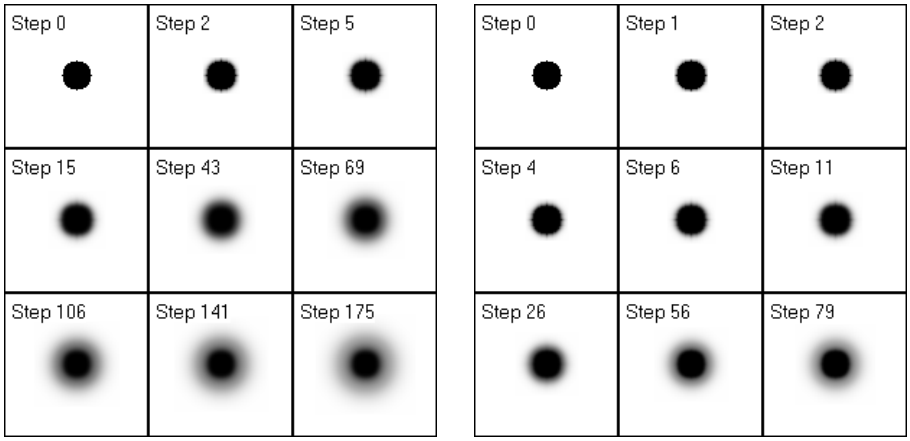


Figure 11: Continuation of the previous figure. Left picture: $a^2 = 0.02$. Right picture: $a^2 = 0.005$. Computer simulation.

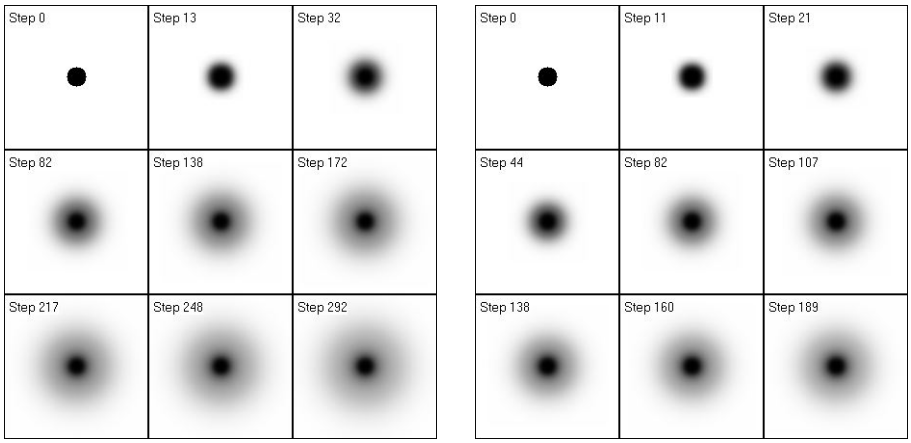


Figure 12: Changing of the resulting image when the water drying rate $\lambda$ increases. Left picture:: $\lambda = 0.05$. Right picture: $\lambda = 0.1$. Computer simulation.

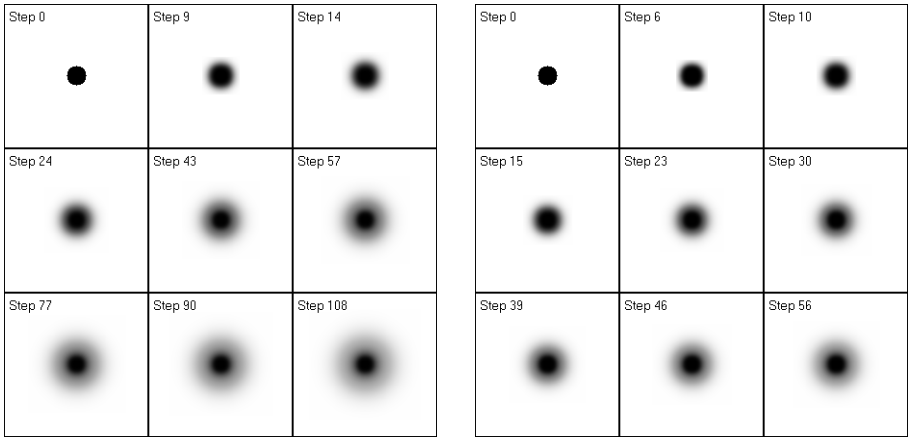


Figure 13: Continuation of the previous figure. Left: $\lambda = 0.2$, right: $\lambda = 0.4$.

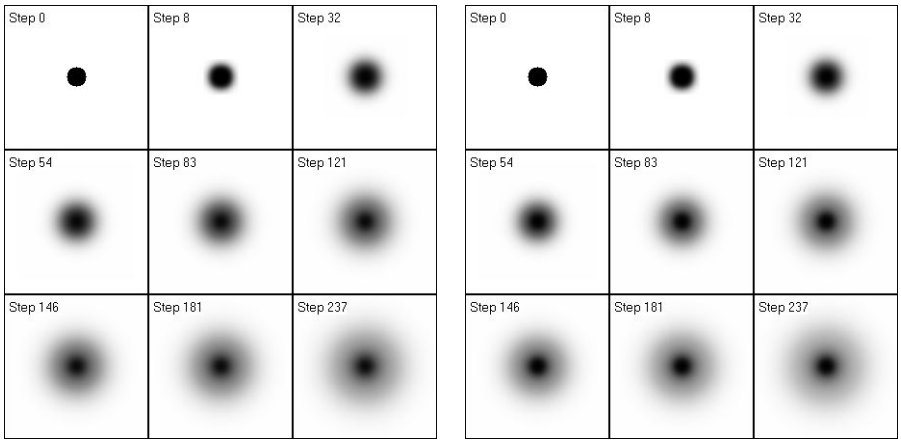


Figure 14: Changing of the resulting image when the carbon quantity in ink (parameter $c$) increases. Left picture: $c = 0.5$. Right picture: $c = 1$. Computer simulation.

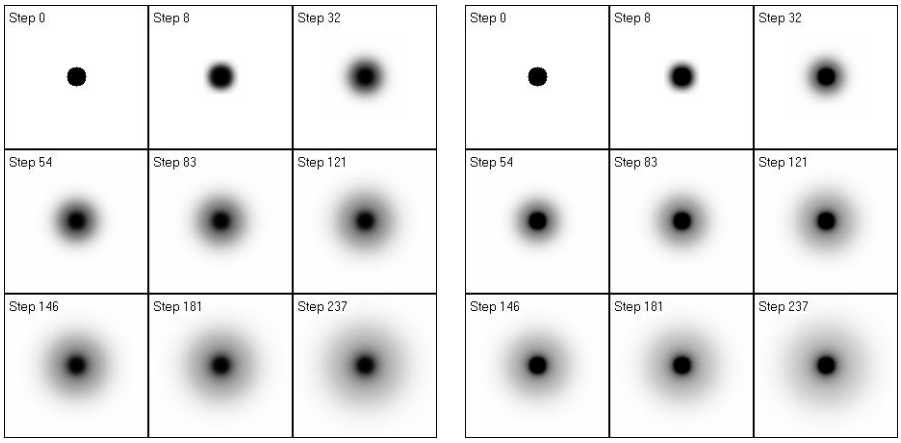


Figure 15: Continuation of the previous figure. Left: $c = 0.5$, right:$c = 1$. Computer simulation.

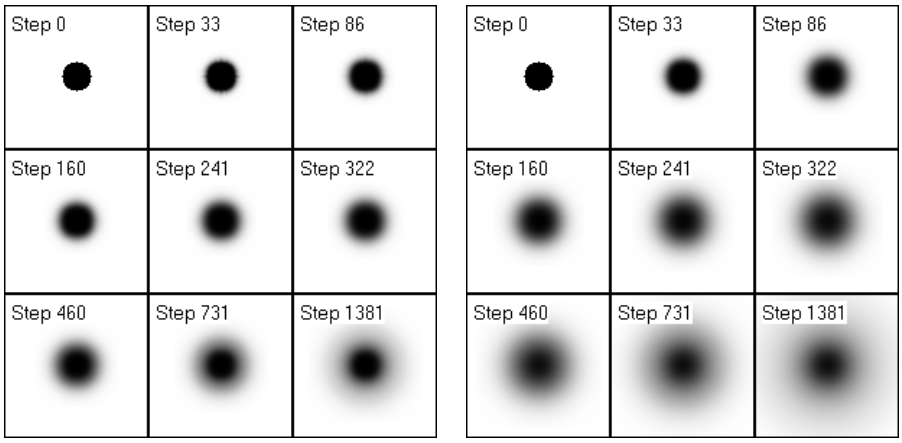


Figure 16: Changing of the resulting image when the parameters $Z_0, Z_1$ increase. In presented images the values $Z_0 = Z_1 = 0.1$ and $Z_0 = Z_1 = 0.4$ were used. All other parameters keep constant values. Computer simulation.

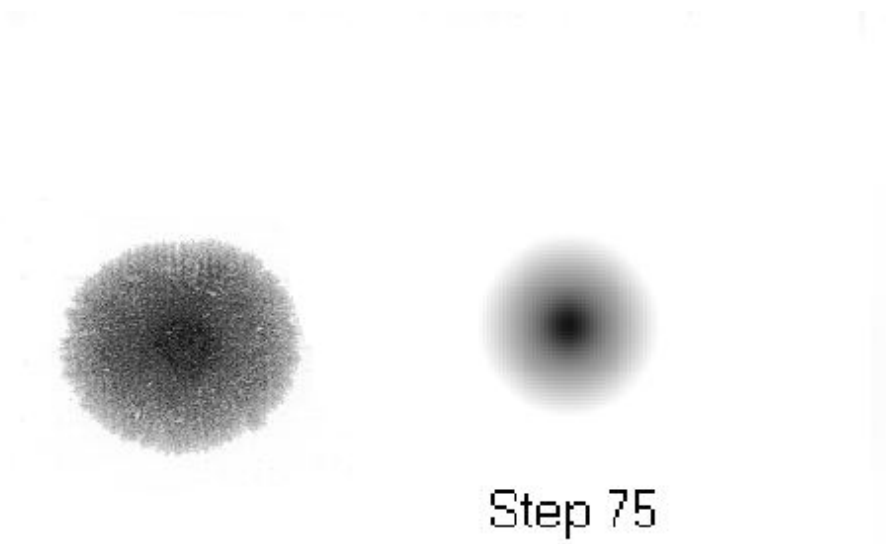


Figure 17: Photo of sumie painting (left) and example of computer simulation (right). Here the fragment of Fig. 7 (right) was used.

## 5 Summary and Conclusions

A new approach to computer animation of complicated phenomenon of diffuse ink painting was proposed in [1]. According to this approach, diffusion of diffuse ink (colloidal liquid) on the surface of the paper should be considered as two separate diffusion processes. In [1] it was shown by simple calculations that the proposed model was able to produce images with singularities in color intensity very similar to real diffuse ink painting images.

In the present paper we carry out new more accurate calculations based on implicit numerical method with alternating direction for solving P.D.E. system (2). The results of calculations show that the proposed model is able to simulate diffuse ink painting. It is possible to control the images by changing values of model parameters. The proposed model could be useful for example in computer software in order to produce computer graphics with different types of "Sumie"-like effects.

## References


[1] T. L. Kunii, G.V.Nosovskij, T.Hayashi "A Diffusion Model for Computer Animation of Diffuse Ink Painting," in *Proc. Computer Animation'95,* Geneva, Switzerland (April 19-21, 1995), IEEE Computer Soc. Press, Los Alamitos, California (1995) 98-102.

[2] Q. Guo, T. L. Kunii, "Modeling the Diffuse Painting of Sumie," *Modeling in Computer Graphics*, Ed. T.L.Kunii (Springer-Verlag, Tokyo, 1991) 229-338.

[3] A. Fournier, "A Simple Model of Ocean Waves," *Computer Graphics,* **20:4** (1986) 75-84.

[4] R. Greene, "The Drawing Prism: A Versatile Graphic Input Device," *Computer Graphics,* **19:3** (1985) 103-117.

[5] J. P. Lewis, "Texture Synthesis for Digital Painting," *Computer Graphics,* **18:3** (1984) 245-252.

[6] D. R. Peachey, "Modeling Waves and Surfaces," *Computer Graphics,* **20:4** (1986) 65-74.

[7] S. Strassmann, "Hairy Brushes," *Computer Graphics,* **20:4** (1986) 225-232.

[8] A.A.Samarskij, "Theory of Difference Schemes," Moscow, Nauka (1989), (in Russian).